Draft
Application of the Geant4 PIXE implementation for space missions
New models for PIXE simulation with Geant4

Georg Weidenspointner, Maria Grazia Pia, and Andreas Zoglauer

***Abstract*—The production of particle induced X-ray emission (PIXE) is an important physical effect that is not yet accurately modelled in Geant4. After providing a brief overview of Geant4 implementations of PIXE up to now, we describe our current effort for improving the Geant4 implementation of PIXE. This research and development activity is part of a larger effort addressing more general aspects of particle transport in Geant4. We illustrate the status of our work by applying a prototype implementation of Geant4 PIXE to a study of the passive shielding of the X-ray detectors of the German eROSITA telescope on the upcoming Russian *Spectrum-X-Gamma* space mission.**

***Index Terms*—Monte Carlo, Geant4, PIXE, ionization.**

I. Introduction

In 1912, Chadwick discovered that energetic charged particles produce X-ray emission in the target material [1]. The origin of the emission lies in the ionization of target material atoms by incident energetic charged particles. Some atoms are ionized by removing an electron from an inner electronic shell; this inner shell vacancy is subsequently filled by an electron from an outer shell. Such an electron transition may give rise to the emission of characteristic X-rays at energies corresponding to the difference in the binding energies of the involved atomic shells.

The application of this characteristic particle induced X-ray emission (PIXE) to non-destructive trace element analysis of materials has first been proposed by Johansson and co-workers in 1970 [2]; today, it is a widely and routinely used technique. The physical process of PIXE may also give rise to unwanted instrumental background X-ray lines in case energetic charged particles reach the detector or passive materials in its vicinity, as is the case for space missions, but also for some laboratory environments.

The physics that needs to be considered for a quantitative simulation of the PIXE process is complex, including energy loss and scattering of the incident charged particle, atomic shell ionization cross sections, and atomic transition probabilities and energies. Several software systems focused on X-ray spectroscopy for material analysis applications of PIXE are available, such as GeoPIXE [3], GUPIX [4]–[6] PIXAN [7], Pixeklm [8], Sapix [9], Winaxil [10] and Witshex [11]; a few cover PIXE simulation [12], [13]. Nevertheless these codes have a limited application scope, as they lack the capability of addressing PIXE simulation in a complex experimental context.

Such comprehensive modelling capabilities are provided in general purpose Monte Carlo systems, such as GEANT 3 [14], MCNP [15]–[17], or FLUKA [18], [19]; however, most of them do not include implementations of PIXE. A partial exception are the Penelope [21] and EGS [22]–[24] electron-photon Monte Carlo codes, which, however, limit themselves to electron impact ionization. With respect to PIXE, the Geant4 simulation toolkit [25], [26] represents the most ambitious attempt at a general implementation of X-ray emission induced not only by electrons, but also by heavy charged particles such as protons, α particles, or ions. However, up to now the Geant4 implementation of PIXE is not yet accurate enough for quantitative studies.

In this paper, we describe our current effort for improving the Geant4 simulation model of PIXE, focusing on the case of proton induced X-ray emission. Once PIXE is correctly modelled for protons, it will be straightforward to extend our strategy to other charged particles. Our Geant4 PIXE research and development (R&D) activity is part of a larger, international effort addressing more general aspects of particle transport, in particular the co-working of condensed-random-walk and discrete transport schemes [27]. The status of our work is illustrated by applying a prototype version of our improved Geant4 PIXE software to studying the passive shield of the X-ray detectors of the German eROSITA (extended Roentgen Survey with an Imaging Telescope Array) telescope on the upcoming Russian *Spectrum-X-Gamma* space mission.

II. PIXE in Geant4

A. General considerations on particle transport

Intrinsically, PIXE is a discrete process, as described in Sec. I. The simulation of the energy loss of a charged particle due to ionization is affected by so-called infrared divergence. This means that in the context of general purpose Monte Carlo

Georg Weidenspointner is with the Max-Planck-Institut für extraterrestrische Physik, Postfach 1603, 85740 Garching, Germany, and with the MPI Halbleiterlabor, Otto-Hahn-Ring 6, 81739 München, Germany (e-mail: Georg.Weidenspointner@hll.mpg.de).

Maria Grazia Pia is with INFN Sezione di Genova, Via Dodecaneso 33, 16146 Genova, Italy (e-mail: MariaGrazia.Pia@ge.infn.it).

Andreas Zoglauer is with the Space Sciences Laboratory, University of California at Berkeley, 7 Gauss Way, Berkeley, CA 94720, USA (e-mail: zog@ssl.berkeley.edu).

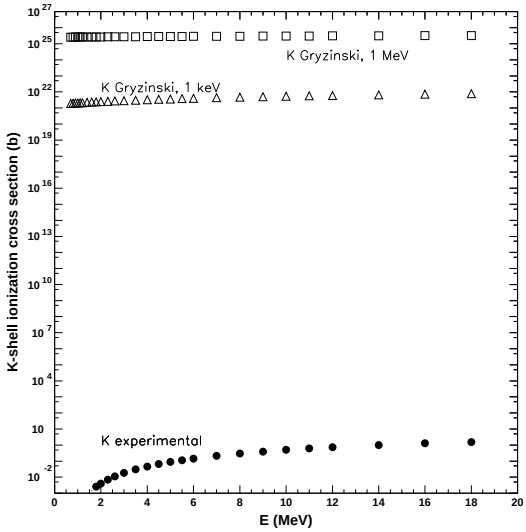

Fig. 1. A comparison of the K shell ionization cross section for Au, implemented in *G4hShellCrossSection* [32], with the experimental reference [33].

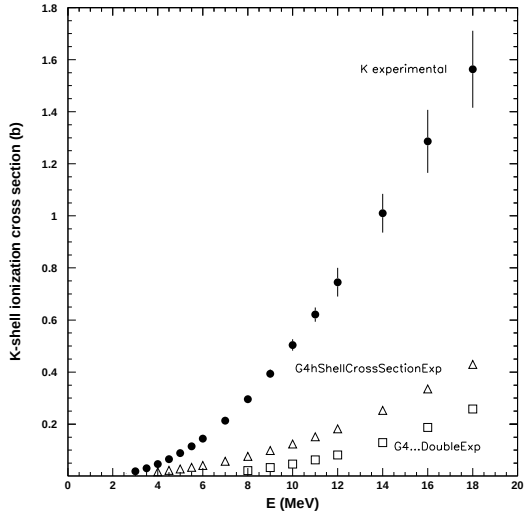

Fig. 2. A comparison of the K shell ionization cross section for Au, implemented in *G4hShellCrossSectionExp* and *G4hShellCrossSectionDoupleExp* [34], [35], with the experimental reference [33].

systems, a discrete treatment of each individual ionization process and subsequent atomic relaxation poses a problem: explicitely considering the production of soft secondary particles may soon become inhibitive, since due to their large number the required computation time becomes excessive.

Infrared divergence is usually handled in general-purpose Monte Carlo codes by adopting a condensed-random-walk scheme for particle transport. In such a scheme, the particle's energy loss and deflection are treated as averaged net effect of many discrete interactions along the step, thereby substituting in the simulation a single continuous process for the many discrete processes that actually occur. In a mixed scheme, like the one adopted by Geant4, two different régimes of particle transport are introduced, which are separated by a threshold for the kinetic energy of the electron that is kicked out of an atom during ionization (the so-called δ ray): all ionizations that result in δ rays below the threshold are treated as a continuous process along the step, the few ionizations that result in δ rays above the threshold are treated as discrete processes.

While this combined condensed-random-walk and discrete particle transport scheme is conceptually appealing and appropriate to many simulation applications, it suffers from drawbacks with respect to the generation of PIXE (as described in Sec. II-C3).

The investigation of software design for different particle transport schemes in the same simulation environment is a main goal of the larger Nano5 program [27], of which PIXE is only a small part. All results in this paper have been obtained with the standard Geant4 particle transport scheme; progress on the simulation of particle transport will be reported elsewhere.

B. Past and present PIXE

Several ionization cross section implementations are available in the Geant4 *low energy* electromagnetic package [28], [29]. Cross sections are used by the hadron ionization process (*G4hLowEnergyIonisation*) to determine the vacancy in the shell occupation produced by impact ionization; this is the first stage to generate X-ray fluorescence emission resulting from atomic relaxation.

The first implementation of PIXE in Geant4 used the theoretical models of Gryziński [30], [31] to compute ionization cross sections for all elements from Hydrogen through Uranium and all atomic shells in the *G4hShellCrossSection* class [32].

However, there was a severe problem in the implemented ionization cross sections. This is illustrated in Fig. 1, comparing the implemented K shell ionization cross section for Au with the experimental reference compiled by Paul & Sacher [33] for incident protons. It is not clear whether the more than 20 orders of magnitude difference is due to an error in the implementation or in the theory or both, but clearly this implementation was inadequate.

A new set of K shell ionization cross sections for incident protons was implemented in *G4hShellCrossSectionExp* and *G4hShellCrossSectionDoupleExp* [34], [35]. This time the cross sections were based on the experimental Paul & Sacher compilation [33] covering the elements Be through U. Two different algorithms were used to interpolate the cross section data base, but neither worked and order of magnitude differences remained between the experimental values and their implementation in Geant4 as illustrated for Au in Fig. 2.

Recently, new ionization cross section implementations [36] have been released in version 9.2-beta of Geant4. Those for K shell ionization are based on the experimental Paul & Sacher database [33] and on the ECPSSR (Energy-Loss Coulomb-Repulsion Perturbed Stationary State Relativistic) theory [38]; the cross sections for L shell ionization are based on a semi-empirical approach from [37]. The software correctly represents the input models or data set; nevertheless, it exhibits severe design limitations, which prevent clients to handle the different cross section models either through dynamic or static polymorphism. Due to their design features,

TABLE I
PERFORMANCE EVALUATION OF TWO DIFFERENT IMPLEMENTATIONS OF K SHELL IONIZATION CROSS SECTIONS FROM ECPSSR THEORY AND FROM EXPERIMENT. THE TWO IMPLEMENTATIONS ARE FROM [36] AS INCLUDED IN GEANT4 9.2-BETA FROM JULY 2008 AND FROM OUR CURRENT PIXE PROTOTYPE IMPLEMENTATION. THE PERFORMANCE HAS BEEN EVALUATED ON AN INTEL CORE2 DUO PROCESSOR E6420, 2.13 GZ, 4 GB RAM, BY INSTANTIATING THE CROSS SECTION CLASSES AND MAKING 10^6 CALLS TO THE CROSS SECTION CALCULATION FUNCTIONS.

ECPSSR K shell			
Element	Geant4 9.2-beta	Our Model	Speed Gain Factor
Si	3.86	0.62	5.9
Cu	3.96	0.63	6.3
Cd	4.24	0.62	6.8
Au	5.21	0.64	8.1
Experimental K shell			
Element	Geant4 9.2-beta	Our Model	Speed Gain Factor
Si	112.83	0.63	179
Cu	107.58	0.62	173
Cd	78.68	0.59	133
Au	66.21	0.53	125

these cross section classes are not usable in any Geant4-based simulation. Moreover, as discussed in Section II-C2 and shown in Table I, these implementations charge a significant performance penalty with respect to the models presented in this paper, which would make them inefficient for practical application purposes.

C. Work in progress

1) Software development process: A satisfactory treatment of PIXE in Geant4 requires addressing its specific requirements together with the complexity of charged particle transport schemes in a general-purpose Monte Carlo environment. The design of such a physics model would have implications on the interaction of processes with other Geant4 kernel objects: an investigation of new design schemes, as well as of new software technologies, looks appropriate at this stage to profit of technical advancements since the conception of Geant4's original design in RD44 [39].

We have begun an iterative-incremental software development process [40] based on the Unified Development Process [41] to address this issue. The initial development cycle, described in this paper, is meant to facilitate the investigation of the problem domain through the production of a prototype still in the current Geant4 kernel design scheme: the lessons learned through this prototype will provide concrete elements to address key physics and software design issues in a following development cycle, while the adopted component-based design will provide the ground for re-using components developed at this early stage in future design iterations.

Despite the foreseen intrinsic limitations in the current design scheme, an effort is invested to investigate physics and software modelling features relevant to the accuracy and computational performance of PIXE simulation. The resulting prototype is meant to provide adequate functionality for a subset of realistic use cases, as it is illustrated in section II-C4.

A class diagram of our current PIXE prototype in the Unified Modelling Language (UML) [42] is given in Fig. 3. Paramount for the design is a well defined domain decomposition that clearly reflects the various functionalities involved, such as cross section calculation, application of cross sections for creation of ionization, final state generation, or atomic relaxation. The *G4RDHadronIonisation* class is an improved version initially based on the hadron ionization process currently implemented in the Geant4 low energy electromagnetic package; the originally developed *G4PixeCrossSectionHandler* class is responsible for cross section management and the creation of the initial shell vacancy resulting from hadron impact; the data management subdomain is responsible for cross section data handling and interpolation. The functionality of producing secondary particles following the initial impact ionization is provided by the Geant4 Atomic Relaxation component [43].

Even if presently applied only to proton induced PIXE, this design is suitable to handle PIXE production by electrons, α particles, and heavy ions without requiring any modification: this extension of functionality would just imply the provision of cross section tabulations for such particles in external data files, which would be handled transparently by the current design model (see Sec. II-C2 below).

It is important to note that we forsee an iterative evolution of this design over the course of our PIXE R&D effort.

2) Ionization Cross Sections: We have adopted a data-driven approach for input of ionization cross sections. Tabulations of the cross sections as a function of element, atomic (sub-)shell, and proton kinetic energy are pre-calculated and stored in files; then the required cross sections at any given energy are calculated by interpolation over the tabulated values whenever required.

This approach presents various advantages. It optimizes performance speed, since the calculation of the interpolation is faster than the calculation from complex algorithms implementing theoretical models. The performance of our approach is superior to that of the latest Geant4 PIXE implemention ([36], see Sec. II-B), as is demonstrated in Table I. Our approach also offers flexibility: chosing a cross section model simply amounts to reading the corresponding set of input files; adding a new set of cross section data simply amounts to pre-calculating the corresponding set of input files. Different modelling approaches, like cross sections based on experimental data or theoretical calculations for different shells, can be easily combined for use in a simulation as desired by the user. Finally, the cross section data are transparent: the files are accessible to the user and human readable.

Various sets of ionization cross sections for K, L, and M shells are currently under study. Theoretical models in different variants include: plain PWBA (Plane Wave Born Approximation) and ECPSSR [38] calculations using the ISICS software [44], [45], ECPSSR with United Atom correction [46], or ECPSSR with corrections for the Dirac-Hartree-Slater nature of the K shell [47]. Experimental ionization cross section data currently include tabulations for the K shell [33]; the experimental database of L shell measurements [48] covers only a limited portion of elements in the periodic system, nevertheless it can be considered as a possible alternative to the theoretical models in a future extension.

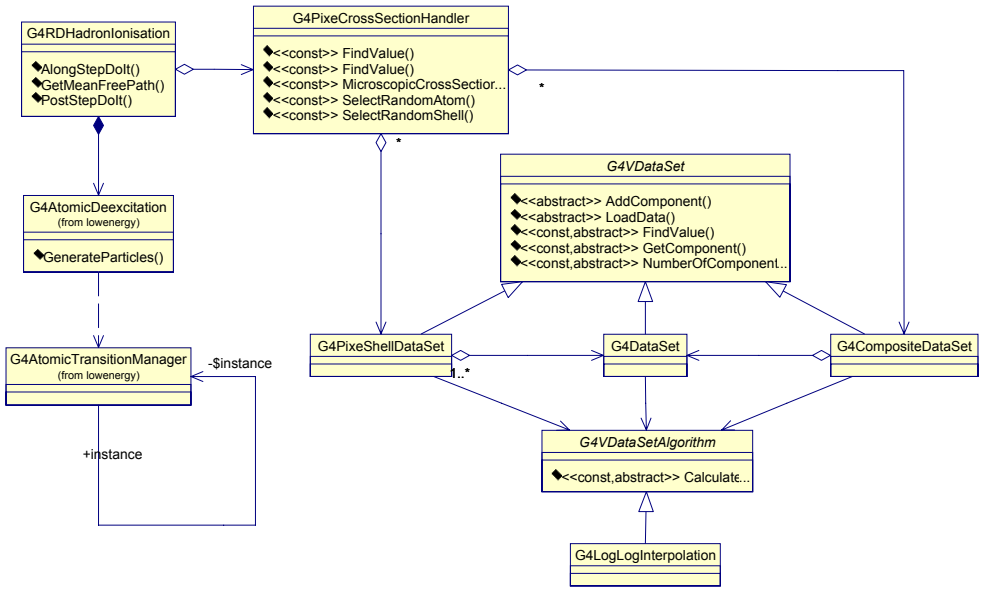

Fig. 3. The Unified Modelling Language [42] class diagram of our current prototype implementation of PIXE, illustrating the main features of the software model.

Comparisons of theoretical and experimental K shell ionization cross sections for Si and Au are shown in Figs. 4 and 5, respectively. Comparisons of L shell ionization cross sections (sum of all sub-shells) for Si, and of L sub-shell cross sections for Au, can be found in Figs. 6 and 7. In general, there is good agreement between different sets of cross sections, but there is also clearly room for further investigations, which are an important aspect of our PIXE R&D effort.

3) Generation of secondary particles: The production of secondary particles resulting from the atomic relaxation of an ionized atom is driven by the *PostStepDoIt* member function of the *G4RDHadronIonisation* class shown in the UML class diagram of Fig. 3.

An example of an X-ray spectrum produced by the PIXE model described in this paper is depicted in Fig. 8, which shows the energy distribution of characteristic photons originating from vacancies produced by proton ionization of Cu in K, L, and M shells, respectively. The relative importance of the different lines appearing in the spectrum is a result of the ionization cross sections for the various shells, combined with the respective probabilities of allowed atomic transitions.

The standard particle transport scheme in Geant4, which combines condensed-random-walk and discrete transport, has been described in Sec. II-A. It is this standard scheme that has been used for the results presented in this paper, despite of its drawbacks for PIXE. One drawback is that atomic relaxation, and therefore the emission of characteristic X-rays or Auger electrons as implemented in the Geant4 Atomic Relaxation package [43], occurs only for those (few) discrete shell vacancies that result from the production of individual δ rays with energies above the respective kinetic energy threshold in the discrete part of the transport scheme. Since no shell vacancies and therefore no atomic relaxations occur in the continuous part, this approach underestimates the yield of X-ray photons. For the same reason, the yield depends on the threshold value for the δ ray kinetic energy. This problem cannot be avoided by simply setting the δ ray production threshold to zero, which effectively would eliminate the continuous part of the energy loss, because analytic approximations in the cross section calculations are only valid for δ ray kinetic energies that are much greater than the mean excitation energy of the material. The dependence of the cross section for discrete ionizations on the δ-ray production threshold energy is illustrated in Fig. 9.

Another drawback of the current transport scheme is that the cross section for discrete ionization, i.e. for production of a δ ray, is calculated in Geant4 from a model for energy loss that is independent of the shell ionization cross sections. The decision whether discrete δ rays are produced during a particle transport step in the simulation is based on the secondary production threshold defined in the user application. The decision in which (sub-)shells the corresponding vacancies have been produced to subsequently model atomic relaxation must be made using available data on shell ionization cross sections. These shell ionization cross sections are currently not available for atomic shells N and higher, consequently this information is incomplete for heavy elements. In such cases one cannot calculate a total ionization cross section based on individual shell contributions. Similarly, once the ionization process has been determined to occur, one cannot apportion the probability for the creation of a vacancy in a given shell.

One possible makeshift solution is to select the (sub-)shell in which discrete ionization occurred based on the relative values of all available (sub-)shell cross sections. Effectively, this means to assume that only those (sub-)shells exist for which cross section data are available, which will result in an over-estimate of the number of vacancies in these (sub-)shells. Although not rigorously correct, this approach has been taken for obtaining the results presented in this paper.

The selection of the shell vacancy for elements with incomplete data on ionization cross sections is still an open

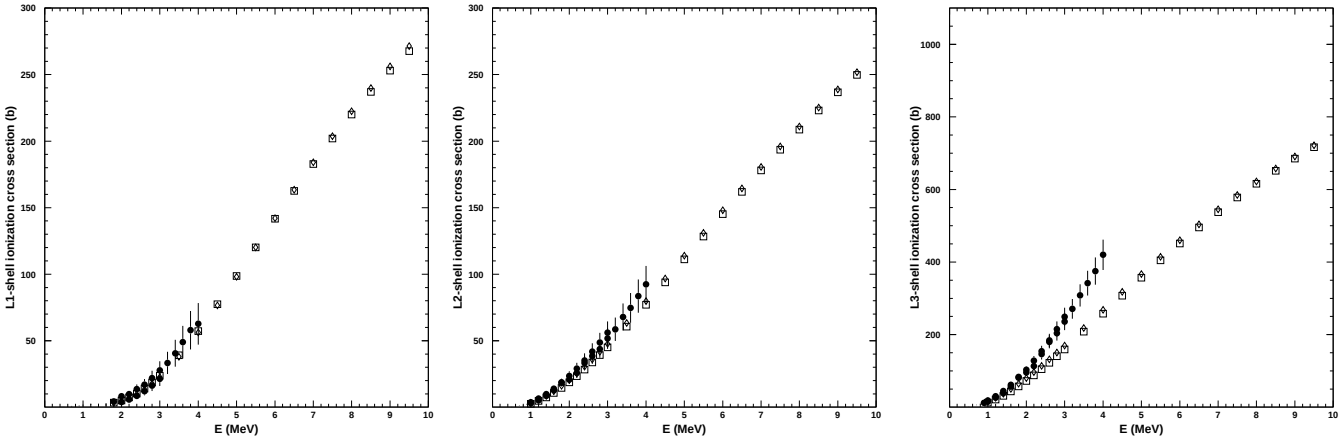

(a) L1 sub-shell (b) L2 sub-shell (c) L3 sub-shell

Fig. 7. A comparison of different sets of Au L sub-shell ionization cross sections for incident protons: ECPSSR/ISICS calculation (squares), PWBA calculation (diamonds), experimental data (filled circles) from Orlic et al. [48].

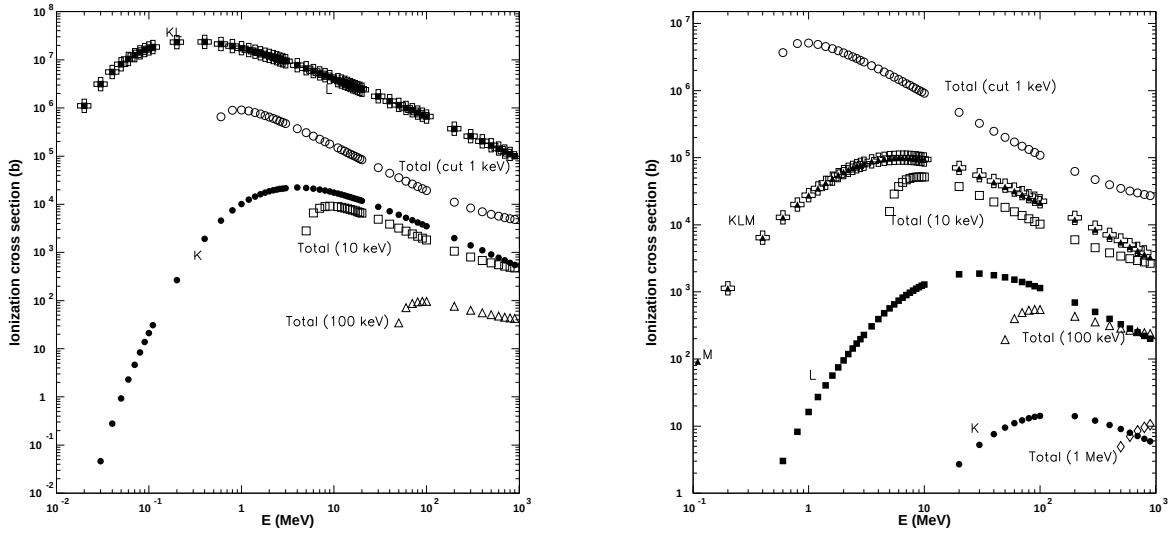

(a) Si (b) Au

Fig. 9. An illustration of the effect of the δ ray production threshold on the discrete part of the ionization cross section. The filled symbols represent ionization cross sections for individual shells (summed over all sub-shells) from an ECPSSR/ISICS calculation: K shell (filled circles), L shell (filled squares), and M shell (filled triangles). For both elements, the sum of all ECPSSR/ISICS shell cross sections is plotted with open crosses (K+L for Si; K+L+M for Au. The total cross section for the discrete part of ionizations as computed in Geant4 is depicted with open triangles for different δ ray production thresholds.

issue, which has not found a satisfactory solution in other Monte Carlo systems either. For instance, the Penelope code treats fluorescence emission resulting from electron impact ionization as an independent discrete process; however, this strategy may lead to negative dose computations in spatial regions of the experimental setup that are subject to large statistical fluctuations [49].

To improve this situation, we are investigating whether ionization cross sections can be computed from theoretical models for all atomic shells. In addition, improvements of the existing and alternative particle transport schemes are investigated in the context of the Nano5 project.

4) An application of our PIXE prototype implementation: We illustrate the status of our work by applying our current Geant4 PIXE prototype implementation to a study of the passive shielding of the X-ray detectors of the eROSITA telescope. The purpose of the passive shielding is to prevent abundant low-energy cosmic-ray particles from reaching the detectors and thus from causing radiation damage. In the shielding, the incident cosmic rays lose energy primarily through ionization, inevitably producing X-ray fluorescence photons in the process. Of particular interest are cosmic rays with sufficient energy (e.g. protons with $E_{\rm kin} \gtrsim 120$ MeV) to penetrate the shield, because these will produce ionization throughout the shield's full volume, including the inner region from which X rays can escape to reach the detector. An important aspect of the design of the passive shielding is to minimize the instrumental background due to the fluorescence

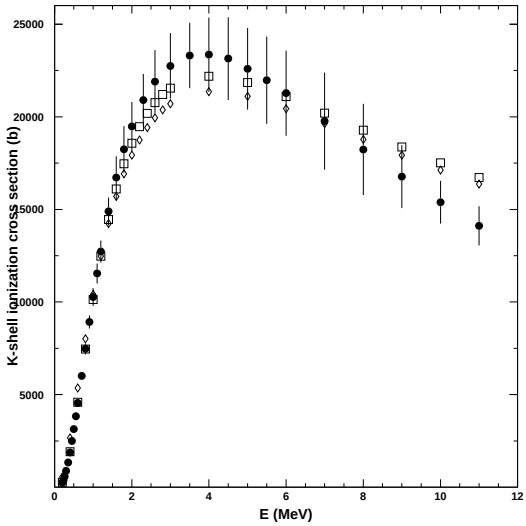

Fig. 4. A comparison of different sets of Si K shell ionization cross sections for incident protons: ECPSSR/ISICS calculation (squares), PWBA calculation (diamonds), experimental data (filled circles) from Paul & Sacher [33].

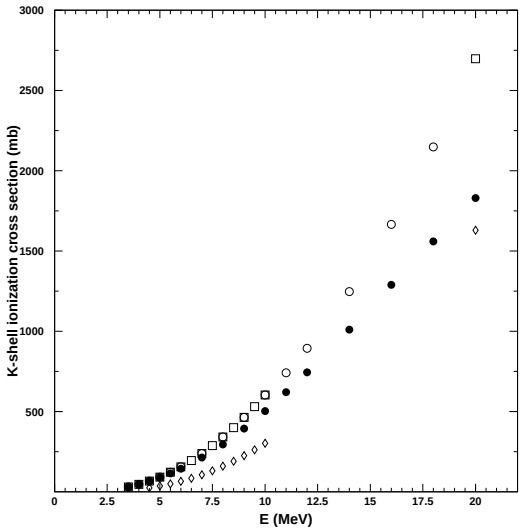

Fig. 5. A comparison of different sets of Au K shell ionization cross sections for incident protons: ECPSSR/ISICS calculation (squares), interpolated from ECPSSR/ISICS tabulation (open circles), PWBA calculation (diamonds), experimental data (filled circles) from Paul & Sacher [33].

lines.

In a first test, we compared the fluorescence lines for three different shielding designs: 3 cm Cu, 3 cm Cu with 1 mm Al, and 3 cm Cu with 1 mm of both Al and B_4C. The different layers are arranged such that the highest Z material is on the outside, and the lowest Z material is on the inside (graded Z shield). A comparison of the fluorescence lines due to ionization by 200 MeV protons, depicted in Fig. 10, demonstrates that qualitatively our PIXE prototype implementation is working properly (see also Fig. 8): protons produce the expected fluorescence lines with correct relative strengths.

We are now working on making the necessary improvements to obtain not only qualitatively, but also quantitatively correct results. A main issue is the lack of PIXE from the continuous

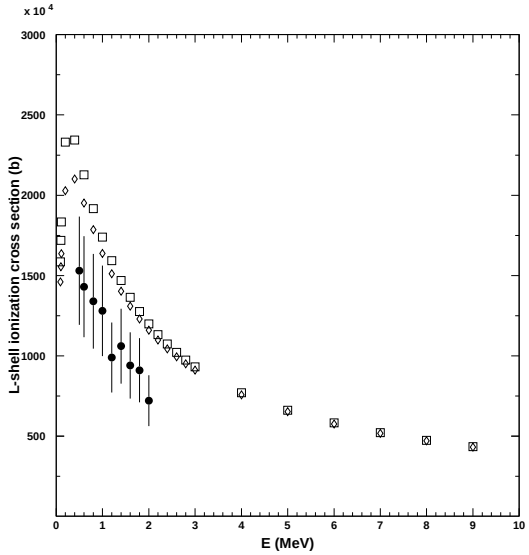

Fig. 6. A comparison of different sets of Si L shell ionization cross sections (summed over all sub-shells) for incident protons: ECPSSR/ISICS calculation (squares), PWBA calculation (diamonds), experimental data (filled circles) from Orlic et al. [48].

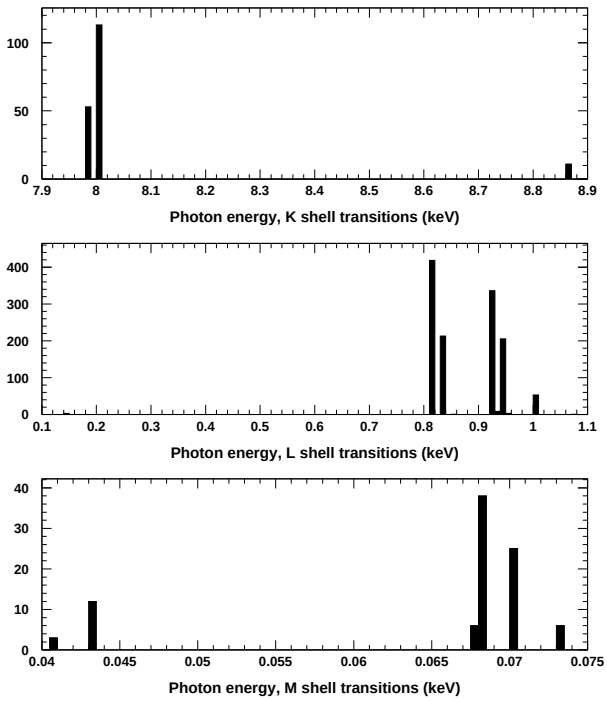

Fig. 8. X-ray spectrum produced by proton ionization of Cu respectively in K, L and M shells; the energy of primary protons is uniformly distributed between 1 keV and 10 MeV.

part of the energy loss and the resulting dependence of the fluorescence line yield on the δ ray production threshold (see Sec. II-C3).

III. Summary and prospects

The production of particle induced X-ray emission is an important physical effect that is not yet accurately modelled

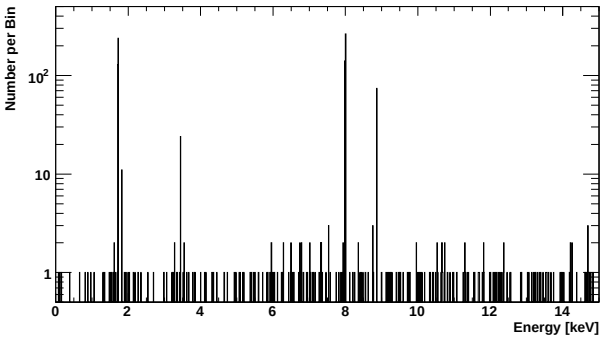

(a) Cu Shield

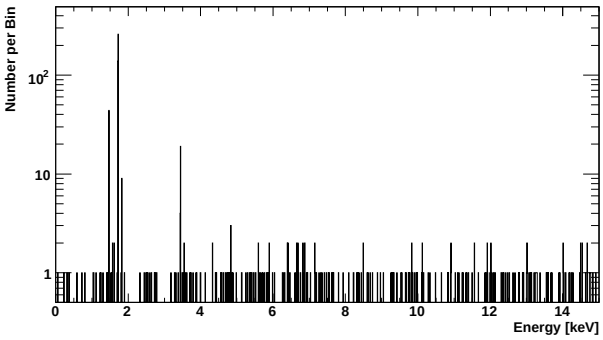

(b) Cu-Al Shield

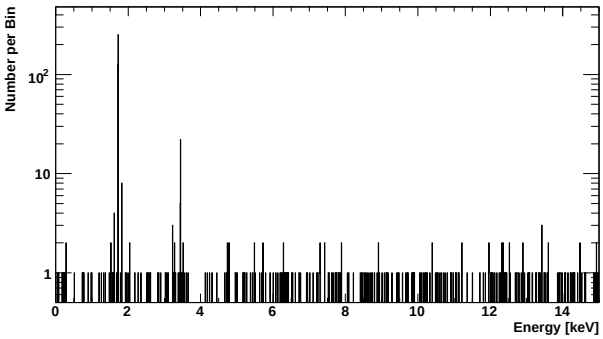

(c) Cu-Al-B_4C Shield

Fig. 10. A comparison of the fluorescence background due to ionization by 200 MeV protons for three different eROSITA X-ray detector shielding designs. The spectra represent the sum of all detector pixel spectra. In case of a pure Cu shield (a), strong Cu K_α and K_β fluorescence lines at about 8.0 and 8.9 keV are present in the background spectrum. In case of a combined Cu-Al shield (b), the Cu fluorescence lines are absorbed in Al, but ionization in Al gives rise to a clear Al K_α fluorescence line at about 1.5 keV. In case of the full graded Z shield configuration (c), the B_4C layer absorbs the Al line, but at the same is not a source of significant fluorescence lines, which is expected due to the low fluorescence yield of these light elements.
For all three cases, the lines around 1.7 keV are due to secondaries from K shell ionization in the Si detector, the line around 3.4 keV is due to Si K_α pile-up in the detector.

in Geant4. After describing the limitations from which Geant4 PIXE implementations suffered until now, we discussed our ongoing R&D effort for improving the treatment of PIXE in Geant4. Our activities include a re-design of the software model, the creation of an extended and improved data base of shell ionization cross sections as well as ameliorations of the application of the cross sections, and investigations into improved particle transport schemes. Our PIXE R&D is only a small part of the larger, international Nano5 program [27], which is mainly aimed at investigating software design for different particle transport schemes in the same simulation environment. We also describe our current Geant4 PIXE prototype implementation, which represents our initial development cycle. As a proof of concept, we applied our PIXE prototype to a study of the passive shielding of the X-ray detectors of the German eROSITA telescope on the upcoming Russian *Spectrum-X-Gamma* space mission.

While our prototype is working qualitatively, a number of improvements are still necessary before it can be used for a quantitative treatment of PIXE with acceptable accuracy. We are investigating further refinements of available shell ionization cross sections, in particular the possibility of obtaining cross sections for atomic shells higher than M, with the goal of building a data base that includes all (sub-)shells for all elements. In addition, we are investigating ways to extend and validate the ionization cross section data base to proton energies beyond a few tens of MeV. Improving particle transport is a crucial aspect of our PIXE R&D that we pursue in the context of the larger Nano5 project [27].

Once proton induced X-ray emission has been correctly implemented in Geant4, it will be straightforward to extend our strategy to other charged particles. After subjecting our PIXE implementations to a thorough validation and verification procedure, we will make them available to the public.

ACKNOWLEDGMENT

The authors thank the INFN Genova Computing Service (A. Brunengo, M. Corosu, P. Lantero, and F. Saffioti) for technical support throughout the project, and U. Bratzler for helpful clarifications concerning the PIXE model presentation at the 2008 IEEE Nuclear Science Symposium.

REFERENCES

[1] J. Chadwick, Phil. Mag. 24, 594, 1912
[2] T. B. Johansson, R. Akselsson, and S. A. E. Johansson, "X-ray analysis: elemental trace analysis at the 10^{-12} g level", *Nucl. Instrum. Meth.*, vol. 84, no. 1, pp. 141-143, 1970.
[3] C. G. Ryan, D. R. Cousens, S. H. Sie, and W. L. Griffin, "Quantitative analysis of PIXE spectra in geoscience applications", *Nucl. Instrum. Meth. B*, vol. 49, no. 1-4, pp. 271-276, 1990.
[4] J. A. Maxwell, J. L. Campbell, and W. J. Teesdale, "The Guelph PIXE software package", *Nucl. Instrum. Meth. B*, vol. 43, no. 2, pp. 218-230, 1989.
[5] J. A. Maxwell, W. J. Teesdale, and J. L. Campbell, "The Guelph PIXE software package II", *Nucl. Instrum. Meth. B*, vol. 95, no. 3, pp. 407-421, 1995.
[6] J. L. Campbell, T. L. Hopman, J. A. Maxwell, Z. Nejedly, "The Guelph PIXE software package III: Alternative proton database" *Nucl. Instrum. Meth. B*, vol. 170, pp. 193-204, 2000.
[7] E. Clayton, "PIXAN, the Lucas Heights PIXE analysis computer package", Australian Nuclear Science and Technology Organisation, AAEC/M113, 1986.
[8] G. Szabo and I. Borbely-Kiss, "PIXYKLM computer package for PIXE analyses" *Nucl. Instrum. Meth. B*, vol. 75, no. 1-4, pp. 123-126, 1993.
[9] K. Sera and S. Futatsugawa, "Personal computer aided data handling and analysis for PIXE", *Nucl. Instrum. Meth. B*, vol. 109-110, pp. 99-104, 1996.
[10] B. Vekemans, K. Janssens, L. Vincze, F. Adams, and P. Van Espen, "Analysis of X-ray Spectra by Iterative Least Squares (AXIL): New Developments", *X-ray spectrometry*, vol. 23, no. 6, pp. 278-285, 1994.

[11] A.D. Lipworth, H.J. Annegarn, and M.A. Kneen, “Advanced, enhanced HEX program for PIXE”, *Nucl. Instrum. Meth. B*, vol. 75, no. 1-4, pp. 127-130, 1993.

[12] K. K. Loh, C. H. Sow, I. Orlic and S. M. Tang, “Computer simulation of PIXE and μ-PIXE spectra for inhomogeneous thick target analysis”, *Nucl. Instrum. Meth. B*, vol. 77, no. 1-4, pp. 132-136, 1993.

[13] C. Pascual-Izarra, N.P. Barradas, and M. A. Reis, “LibCPIXE: A PIXE simulation open-source library for multilayered samples”, *Nucl. Instrum. Meth. B*, vol. 249, no. 1-2, pp. 820-822, 2006.

[14] “GEANT Detector Description and Simulation Tool”, CERN Program Library Long Writeup W5013, 1995.

[15] X-5 Monte Carlo Team, “MCNP – A General Monte Carlo N-Particle Transport Code, Version 5”, Los Alamos National Laboratory Report LA-UR-03-1987, Apr. 2003, revised Mar. 2005.

[16] R.A. Forster et al., “MCNP Version 5”, *Nucl. Instrum. Meth. B*,vol. 213, pp. 82-86, 2004

[17] J.S. Hendricks et al., “MCNPX, Version 26c”, Los Alamos National Laboratory Report LA-UR-06-7991, Dec. 2006.

[18] A. Fassò et al., “The physics models of FLUKA: status and recent developments”, in *Proc. Computing in High Energy and Nuclear Physics 2003 Conference (CHEP 2003)*, La Jolla, CA, USA, paper MOMT05.

[19] A. Ferrari et al., “Fluka: a multi-particle transport code”, Report CERN-2005-010, INFN/TC-05/11, SLAC-R-773, Geneva, Oct. 2005.

[20] J. Baro,, J. Sempau, J. M. Fernandez-Varea, and F. Salvat, “PENELOPE: An algorithm for Monte Carlo simulation of the penetration and energy loss of electrons and positrons in matter” *Nucl. Instrum. Meth. B*, vol. 100, no. 1, pp. 31-46, 2005.

[21] Penelope – A code system for Monte Carlo simulation of electron and photon transport, Workshop Proceedings Barcelona, Spain, 4–7 July 2006, ISBN 92-64-02301-1, NEA.

[22] W.R. Nelson, H. Hirayama, and D.W.O. Rogers, “The EGS4 code system”, Report SLAC-265, Stanford Linear Accelerator Center, Stanford, CA, USA, 1985.

[23] I. Kawrakow and D.W.O. Rogers, “The ENSnrc Code System: Monte Carlo Simulation of Electron and Photon Transport”, NRCC Report PIRS-701, Sep. 2006.

[24] H. Hirayama, et al., “The EGS5 code system”, Report SLAC-R-730, Stanford Linear Accelerator Center, Stanford, CA, USA, 2006.

[25] S. Agostinelli et al., “Geant4 - a simulation toolkit” *Nucl. Instrum. Meth. A*, vol. 506, no. 3, pp. 250-303, 2003.

[26] J. Allison, et al., “Geant4 Development and Applications”, *IEEE Trans. Nucl. Sci.*, vol. 53, no. 1, pp. 270-278, 2006.

[27] M. G. Pia, “Nano5: R&D of new architectural design for novel simulation domains”, INFN Internal Document, Genova, July 2008.

[28] S. Chauvie et al., “Geant4 Low Energy Electromagnetic Physics”, in *Proc. Computing in High Energy and Nuclear Physics*, Beijing, China, pp. 337-340, 2001.

[29] S. Chauvie et al., “Geant4 Low Energy Electromagnetic Physics”, in *Conf. Rec. 2004 IEEE Nucl. Sci. Symp.*, N33-165.

[30] M. Gryziński, “Two-Particle Collisions. I. General Relations for Collisions in the Laboratory System”, *Phys. Rev.*, vol. 138, 2A, pp. 305-322, 1965.

[31] M. Gryziński, “Two-Particle Collisions. II. Coulomb Collisions in the Laboratory System of Coordinates”, *Phys. Rev.*, vol. 138, 2A, pp. 322-335, 1965.

[32] S. Dussoni, A. Mantero, I. Ivanchenko, and S. Saliceti, Geant4 source code. Online. Available: http://cern.ch/geant4/support/download.shtml.

[33] H. Paul and J. Sacher, “Fitted empirical reference cross sections for K-shell ionization by protons”, *At. Data Nucl. Data Tab.*, vol. 42, pp. 105-156, 1989.

[34] S. Saliceti, “Studio della Composizione del Pianeta Mercurio: Modelli per l’Emissione di Fluorescenza e la loro Validazione Sperimentale”, MSc. Thesis, Univ. of Genova, 2004.

[35] A. Mantero, “Development and validation of X-ray fluorescence simulation models for planetary astrophysics investigations”, PhD Thesis, Univ. of Genova, 2008.

[36] H. Abdelhwahed, “PIXE Simulation with geant4 new models for cross sections calculation”. Online. Available: http://geant4loweworkinggroup.wikispaces.com/file/view/Haifa-2008.pdf.

[37] I. Orlic, C. H. Sow, and S. M. Tang, “Semiempirical Formulas for Calculation of L Subshell Ionization Cross Sections”, *Int. J. PIXE*, vol. 4, no. 4, pp. 217-230, 1994.

[38] W. Brandt and G. Lapicki, “Energy-loss effect in inner-shell Coulomb ionization by heavy charged particles”, *Phys. Rev. A*, Vol. 23, 1717, 1981.

[39] S. Giani, “GEANT4 : an object-oriented toolkit for simulation in HEP”, CERN Report CERN-LHCC-98-044, Geneva, 1998.

[40] S. Guatelli, et al., “Experience with Software Process in Physics Projects”, in *Conf. Rec. 2004 IEEE Nucl. Sci. Symp.*, N40-8.

[41] I. Jakobson, G . Booch, and J. Rumbaugh, “The Unified Development Process”, Ed. Addison-Wesley, Boston, 1999.

[42] G . Booch, J. Rumbaugh, and I. Jakobson, “The Unified Modelling Language User Guide”, Ed. Boston: Addison-Wesley, 1999.

[43] S. Guatelli et al., “Geant4 Atomic Relaxation”, *IEEE Trans. Nucl. Sci.*, vol. 54, no. 3, pp. 585-593, 2007.

[44] Z. Liu and S.J. Cipolla, “ISICS: A program for calculating K-, L-, and M-shell cross sections from ECPSSR theory using a personal computer”, *Comp. Phys. Comm.*, vol. 97, pp. 315-330, 1996.

[45] S.J. Cipolla, “An improved version of ISICS: a program for calculating K-, L-, and M-shell cross sections from PWBA and ECPSSR theory using a personal computer”, *Comp. Phys. Comm.*, vol. 176, pp. 157-159, 2007.

[46] S.J. Cipolla, “The united atom approximation option in the ISICS program to calculate K-, L-, and M-shell cross sections from PWBA and ECPSSR theory”, *Nucl. Instrum. Meth. B*, vol. 261, pp. 142-144, 2007.

[47] G. Lapicki, “The status of theoretical K-shell ionization cross sections by protons”, *X-Ray Spectrom.*, vol. 34, pp. 269–278, 2005.

[48] I. Orlic, J. Sow, and S.M. Tang, “Experimental L-shell X-ray production and ionization cross sections for proton impact”, *At. Data Nucl. Data Tab.*, vol. 56, pp. 159-210, 1994.

[49] F. Salvat, J. M. Fernandez-Varea, and J. Sempau, “PENELOPE - A Code System for Monte Carlo Simulation of Electron and Photon Transport”, Workshop Proceedings, Issy-les-Moulineaux, France, Data Bank ISBN 92-64-02145, 2003.